Early Onset of Kinetic Roughening due to a Finite Step Width in Hematin Crystallization

Katy N. Olafson, Jeffrey D. Rimer, and Peter G. Vekilov

Phys. Rev. Lett. **119**, 198101 — Published 7 November 2017

DOI: 10.1103/PhysRevLett.119.198101

Early onset of kinetic roughening due to finite step width in hematin crystallization

Katy N. Olafson[1], Jeffrey D. Rimer[1,2,*], and Peter G. Vekilov[1,2,*]

[1]Department of Chemical and Biomolecular Engineering and [2]Department of Chemistry, University of Houston, 4726 Calhoun Road, Houston, Texas 77204-4004, USA.

[*] Corresponding authors

The structure of the interface of a growing crystal with its nutrient phase largely determines the growth dynamics. We demonstrate that hematin crystals, crucial for the survival of malaria parasites, transition from faceted to rough growth interfaces at increasing thermodynamic supersaturation $\Delta\mu$. Contrary to theoretical predictions and previous observations, this transition occurs at moderate values of $\Delta\mu$. Moreover, surface roughness varies non-monotonically with $\Delta\mu$ and the rate constant for rough growth is slower than that resulting from nucleation and spreading of layers. We attribute these unexpected behaviors to the dynamics of step growth dominated by surface diffusion and the loss of identity of nuclei separated by less than the step width w. We put forth a general criterion for the onset of kinetic roughening using w as a critical lengthscale.

Crystallization is an example of a highly non-equilibrium process, in which the flows of mass and energy are governed by dynamic structures comprising a two-dimensional interface between adjacent three-dimensional semi-spaces; it is also a crucial part of innumerable natural and commercialized processes [1-4]. During crystal growth, the structure of its interface with the growth medium dictates the molecular mechanism of solute incorporation, the response of the growth dynamics to temperature and composition gradients, the action of impurities and dopants, and, ultimately, the crystal perfection [5,6]. Crystals growing from a melt are typically non-

faceted. Such interfaces are denoted as rough and exhibit a high density of growth sites, referred to as kinks, Fig. 1(a) [5]. In contrast, the interfaces of most crystals growing from dilute media, such as solutions, follow the lattice planes and are molecularly smooth. Kink sites are rare and located along steps comprising the edges of unfinished crystal layers, Fig. 1(b) [7]. The generation of kinks and the transport of solute to these sites are major factors governing crystallization, leading to growth rates slower by orders of magnitude than those for rough growth [5,8-13].

In equilibrium and at low supersaturation, the selection between a rough and smooth interface is dictated by the ratio of the crystal bond strength ψ to the thermal energy k_BT (k_B, Boltzmann constant; T, temperature) [14,15]. The parameter ψ, in turn, is proportional to the latent heat of crystallization ΔH^o_{cryst} [16]. For melt crystallization, typical ΔH^o_{cryst} values (and the corresponding ψ) are low and the temperatures are high [17], whereas ΔH^o_{cryst} and ψ for growth from solution are higher and T is constrained by the boiling point of the solvent. Numerous classical models relate $\psi/k_BT < 1$ to rough interfaces and $\psi/k_BT > 1$, to faceted crystals [18-20].

Interfaces that are smooth at equilibrium may become rough during growth at elevated supersaturation [21,22]. We observed a smooth to rough transition, Figs. 1(c)–1(f), during the growth of hematin crystals from a biomimetic mixed organic-aqueous solvent [23-25]; for experiment details, see SM at [URL will be inserted by publisher]. Hematin crystallization is the main pathway employed by malaria parasites to sequester toxic hematin, released during hemoglobin digestion [26]; its inhibition is considered the most successful target for antimalarial drugs [27]. Here, we use *in situ* atomic force microscopy (AFM) to show that the transition

occurs at supersaturation significantly lower than that predicted by published criteria [9,10,14,22,28-31]. We demonstrate that the transition is controlled by the balance between nucleation of new layers and their coalescence into smooth surfaces. We highlight the significance of solute incorporation into kinks from the surface (and not directly from the solution) for the early onset of kinetic roughness.

Previous observations of hematin crystals in undersaturated and moderately supersaturated solutions conditions have revealed that they are faceted with smooth faces and grow by layers, generated by two-dimensional (2D) nucleation, which then spread and merge to cover the surface (Fig. 1c) [24,32]. The smooth surface agrees with the predictions of the above criteria for interface structure of crystals near equilibrium with the solution. The latent heat of crystallization is ΔH^{o}_{cryst} = –37 kJ mol^{-1} [24]. The hematin crystal structure [33] in SM [URL will be inserted by publisher]) implies that the coordination number of the hematin molecules in the crystal is Z = 8. The mean $\psi = 2\left|\Delta H^{o}_{cryst}\right|/ZN_A \cong 3.8k_BT$ (N_A, Avogadro's number). At $\Delta\mu > 0.8k_BT$ (the definition of $\Delta\mu$ is discussed in the SM at [URL will be inserted by publisher]) the surface becomes rough, Fig. 1(d), and this roughness is preserved at $\Delta\mu$ as high as 1.48 k_BT, Figs. 1(e) and (f).

Criteria for the onset of kinetic roughening include vanishing R_c (critical radius of the 2D nucleus) and the corresponding barrier for 2D nucleation, ΔG^*, at high supersaturation [9,10,29-31]. According to classical nucleation theory (CNT), applied to 2D islands on a crystal substrate [34], island nuclei form as a result of fluctuations of the concentration of molecules on the surface. Islands of radius R, illustrated in Fig. 2(a), smaller than R_c are more likely to dissolve, whereas those exceeding R_c have a high probability to grow. The dependence $R_c(\Delta\mu)$ is governed

by the Gibbs-Thomson relation, according to which $R_c = \Omega\gamma/\Delta\mu$ (where γ is the surface free energy of the step edge and Ω is the volume of one molecule in the crystal) [5]. In turn, R_c relates to $\Delta G^* = \pi\gamma R_c h$, where h is layer thickness, often equal to one lattice parameter a. If ΔG^* falls below the thermal energy $k_B T$, nucleation of new layers is barrier-free (analogous to spinodal decomposition) and induces a rough growth interface.

Individual criteria diverge in their identification of the processes that cause a decrease in ΔG^* and R_c. Several authors postulate vanishing γ at high $\Delta\mu$ due to high step configurational entropy induced by fast solute association [9,29], akin to the vanishing γ between liquids and gasses at the critical point [5,35]. The elevated entropy compensates for the enthalpy contribution to γ if $\psi < 2.5 k_B T$, which corresponds to $\Delta H^o_{cryst} < 18$ kJ mol^{-1} for the assumed Kossel crystal structure [29]. This mechanism does not apply to the roughening transition observed in Fig. 1 because ΔH^o_{cryst} for hematin is significantly higher than this limit. Other criteria predict kinetic roughening if R_c is reduced below a threshold length at high $\Delta\mu$. Two characteristic lengthscales have been put forth: the correlation length of the step contour ξ, illustrated in Fig. 2(b) [36], or the size of one solute molecule a [10,30,31].

Under specific conditions, surfaces may be covered by trains of parallel steps, Fig. 2(b). The criteria that treat roughening transitions on such interfaces predict the onset of surface roughness at supersaturation where the interstep separation ℓ becomes shorter than the step correlation length ξ [14] or the step width w, Fig. 2(b) [5]. Trains of parallel steps have not been observed on growing hematin crystals [24,32]. Irrespective of the roughening mechanism, it is generally accepted that, owing to a consistently increasing 2D nucleation rate in the regime of rough growth, the interface roughness will increase monotonically with supersaturation

[6,13,22]. Furthermore, it is expected that rough surfaces grow with significantly higher rate constants than smooth surfaces [8,11-13].

To elucidate the mechanism of kinetic roughening, we quantified the surface roughness of hematin interfaces represented in Figs. 1(c)–1(f). We evaluated the root mean squared roughness R_q within surface segments of area Σ, Figs. 2(c)–2(f). The smooth surface in Fig. 1(c) reveals mostly R_q values corresponding to the presence of one or two steps in the sampled surface segment, Fig. 2(c). The rough surfaces in Figs. 1(d)–1(f) exhibit height differences of up to 4.5 nm, indicating a large disparity in heights of the analyzed profiles, Figs. 2(d)–2(f). Surprisingly, $\overline{R_q}$ averaged over all sampled surfaces passes through a maximum and reaches, at high supersaturations, values that are lower than those for smooth interface at $\Delta\mu = 0.32k_BT$ in Fig. 1(c). Statistical analysis reveals that this non-monotonic trend is independent of Σ, as discussed in the SM at [URL will be inserted by publisher].

Decreasing $\overline{R_q}$ with increasing $\Delta\mu$ contradicts theoretical predictions [6,22] and previous experimental observations [12,13,37]. It is not a consequence of limited imaging resolution since the pixel size on the images in Figs. 1(c)–(f) is about 3 nm, close to the hematin molecular size of 1.2 nm [33]. Moreover, AFM tip curvature artifacts do not constrain the resolution for objects with surface height variations < 5 nm [38,39], and the highest observed height variation in the profiles used to calculate R_q is 4.5 nm. The decreasing $\overline{R_q}(\Delta\mu)$ trend suggests that the characteristic lengthscale of the surface *decreases* after the onset of roughening, in direct contradiction with the models correlating roughening with vanishing ΔG^* and R_c, in which the characteristic lengthscale of a rough surface is a [40-43].

To further test the applicability of these models to hematin growth, we correlate the observed kinetic roughening, Figs. 1(c)–1(f) and 2(c)–(g), with the $R_c(\Delta\mu)$ dependence. For the highly anisotropic hematin crystals [32,33] we define R_c as an azimuthally averaged half-width of the 2D nuclei and determine it from observations of the size and shape fluctuations of newly nucleated islands, as illustrated in Figs. 3(a)–3(f) [24]. The $R_c(\Delta\mu)$ data comply remarkably well with the prediction of the Gibbs-Thomson relation using $\Omega = 0.708$ nm^3 [33] and $\gamma = 23$ mJ m^{-2}, independently determined using the Turnbull rule and ΔH^o_{cryst} [24], Fig. 3(g). In the SM at [URL will be inserted by publisher], we demonstrate that this γ represents an azimuthal average and justify its relation with R_c *via* the Gibbs-Thomson law. Extrapolating the $R_c(\Delta\mu)$ dependence reveals that at the onset of roughening, at $\Delta\mu = 0.80 k_B T$, $R_c \cong 4$ nm. Recognizing that the surface area per molecule is ca. 0.5 nm^2, an island of such radius would contain approximately 100 molecules. Creating such islands would require a significant free energy expense. This conclusion excludes vanishing ΔG^* as a mechanism of kinetic roughening. Furthermore, steps on hematin (100) faces exhibit relatively long straight segments, Figs. 1(c) and 3(h), indicating that the step correlation length ξ may be of order tens of nanometers, thus eliminating the relation $R_c < \xi$ as a viable threshold for roughening.

Here, we put forth an alternative mechanism of surface roughening at elevated supersaturations. We assume that the surface would be rough if two conditions are met: First, 2D nuclei are separated by distances shorter than the step width w (finite w reflects step contour fluctuations due to the creation and annihilation of kinks, which stabilize the step via increased entropy [5,14,18]). Such high nuclei density hinders the distinction between steps and terraces and the identification of individual crystal layers [44]. Second, the preservation of roughness

during growth requires that the layers spread and merge within time scales longer than those needed for the formation of nuclei belonging to the next crystal layer. The characteristic time of the former process is w/v, and that of the latter is $(Jw^2)^{-1}$ (where J is the rate of 2D nucleation of new crystal layers, and v is the step velocity) [5,20,45,46]. The surface will be rough when $(Jw^2)^{-1} < w/v$ (or $Jw^3/v > 1$) and smooth when $Jw^3/v < 1$. Determinations of J and v from *in situ* AFM reveal that at $\Delta\mu = 0.32k_BT$, $J \approx 10^{13}$ m^{-2} s^{-1} and v of closely spaced steps is about 0.05 nm s^{-1} [24,32]. The step width w is about 5 nm, Fig. 3(h), yielding $Jw^3/v \approx 0.02$. This corresponds to a smooth interface, as seen in Fig. 1(c).

In compliance with CNT, J increases exponentially with $\Delta\mu$ and reaches a value of 3.5×10^{14} m^{-2}s^{-1} at $\Delta\mu = 0.58k_BT$ [32]. We extrapolate J to a value of 10^{15} m^{-2}s^{-1} at $\Delta\mu = 0.80k_BT$. For steps separated by more than 180 nm, v increases linearly with c_H [24,32]. Previous experiments have demonstrated that the pathway of hematin molecules from the solution to kinks includes a state of adsorption on the terraces between steps and 2D diffusion towards the kinks [32]. The competition for nutrient supply between adjacent steps retards v, as observed for two steps separated by about 50 nm and growing towards each other, Figs. 4(a)–(e), with average $v \approx$ 0.05 nm s^{-1}. Under identical conditions, steps separated by more than 180 nm move with $v = 0.12$ nm s^{-1} [24,32]. At step separations ℓ shorter than 180 nm, the $v(c_H)$ correlation exhibits a plateau in at $v \approx 0.05$ nm s^{-1}, as demonstrated in the SM at [URL will be inserted by publisher] [32]. At this approximate value of v, the relation $Jw^3/v \approx 1$ signifies the onset of kinetic roughening at $\Delta\mu = 0.80k_BT$.

To elucidate the consequences of surface roughening on the normal growth rate V of a crystal, we consider the face kinetic coefficient β_{face}, defined from the correlation $V = \beta_{face}\Omega(c_H -$

c_e) [5], Fig. 4(f). This β_{face} is proportional to the effective first-order rate constant k for incorporation of hematin molecules into crystals $\beta_{face} = ak$. Surprisingly, β_{face} for rough growth is comparable to that at very low supersaturations, where growth is constrained by slow J. At intermediate supersaturations, where J is fast, β_{face} for smooth growth is significantly faster than that in the rough regime, in direct contradiction to numerous theoretical predictions [5,8-10] and previous experimental observations [11-13,47]. The slow V in the rough regime, which occurs despite rapid nucleation of new layers, is likely due to the slow velocity v of step spreading.

On a smooth interface, the surface diffusion pathway is selected because it induces significantly faster growth rate (v and V) than the alternative direct incorporation of solute into kinks [48]. During rough growth, when the characteristic surface lengthscale is comparable to the molecular size, terraces are rendered unavailable for solute adsorption and direct incorporation is the only pathway from the solution to the kinks. This pathway reduces β_{face} below values observed for layer-by-layer growth. The somewhat larger β_{face} at c_H = 0.40 mM (where $\Delta\mu = 0.92k_BT$) is consistent with islands separated by terraces of width w, which allow solute adsorption on terraces followed by surface diffusion to incorporate into step sites. The availability of surface incorporation pathways leads to faster v and V. The incorporation pathway through adsorption on the surface enables two additional unexpected behaviors discussed above. The early onset of roughening at supersaturations where R_c is large and the maximum in $\overline{R_q}$ are both due to the weak $v(c_H)$ dependence associated with this pathway, leading to a steep increase of the ratio Jw^3/v to values above 1 at moderate $\Delta\mu$.

Published observations of kinetic roughening with the proteins lysozyme and glucose isomerase [13,47], which grow via a similar solute incorporation pathway, are consistent with the

proposed transition scenario. In lysozyme growth, step retardation occurs at $\ell < 2\ \mu m = 600a$ [49], indicating a more pronounced step supply field overlap than with hematin [13]. Correspondingly, the surface roughens at $\Delta\mu = 0.4k_BT$ [13], about half the value for hematin. The surface free energy is about 0.5 mJ m^{-2} [50] and, with $\Omega = 2\times10^{-26} m^3$, R_c reaches a = 3.5 nm at about $\Delta\mu = 0.6k_BT$. Hence, surface roughness should increase at values $\Delta\mu$ greater than this latter threshold, in agreement with reported observations [13]. With glucose isomerase, step retardation was minimal and recorded at separations < 70 nm ≅ $7a$ [51]. In combination with a slow increase of J with $\Delta\mu$, fast v leads to roughening at $\Delta\mu = 5.0k_BT$, which coincides with where ΔG^* vanishes [47].

In summary, we show that hematin crystals transition into a rough growth regime at less than expected supersaturations. The early onset of roughening is enabled by the surface diffusion mechanism, which results in slower step velocity at the shorter interstep distances at high supersaturation. Slow layer spreading reveals the surface roughens at lengthscales significantly longer than those for vanishing nucleation barrier, which are assumed to be the trigger for kinetic roughening in the majority of published models. We propose that the interface roughens when the spacing between island nuclei falls below the step width and slow island growth hinders the merging of layers. A numerical criterion based on this scenario accurately predicts the hematin roughening transition and is consistent with available data for two other recently studied crystalline materials.

The slow β_{face} in the rough growth regime may relate to the high efficacy of antimalarial drugs that inhibit hematin layer growth [52,53]. After cessation of layer-by-layer growth due to drug action, the accumulation of hematin, continuously released by hemoglobin digestion [54],

would force the system into rough growth, as illustrated in SM [URL will be inserted by publisher]. It is feasible that the roughening of the crystal surface removes the preferred adsorptions sites of the drugs and allows crystallization to proceed uninhibited. If β_{face} for rough growth were greater than that for faceted growth, the accumulated toxic hematin would be consumed, preventing the demise of the parasite[55]. Slow β_{face}, by contrast, supports continued increase of c_H to values above the toxic level, as schematically illustrated in SM [URL will be inserted by publisher], and contributes to effectiveness of the drugs.

We thank E. Vlieg for helpful discussions and suggestions. This work was supported by NIH (Grant 1R21AI126215-01), NSF (DMR-1710354), NASA (NNX14AD68G and NNX14AE79G), and The Welch Foundation (Grant E-1794).

[1] J. W. Mullin, *Crystallization, Fourth Edition* (Butterworth-Heinemann, 2001).
[2] S. Weiner and P. M. Dove, Reviews in Mineralogy and Geochemistry **54**, 1 (2003).
[3] A. S. Myerson, *Handbook of Industrial Crystallization: Second Edition [Paperback]* (Butterworth-Heinemann, Woburn, MA, 2001).
[4] J. P. K. Doye and W. C. K. Poon, Current Opinion in Colloid & Interface Science **11**, 40 (2006).
[5] A. A. Chernov, *Modern Crystallography III, Crystal Growth,* (Springer, Berlin, 1984).
[6] J. D. Weeks and G. H. Gilmer, in *Advances in Chemical Physics* (John Wiley & Sons, Inc., 2007), pp. 157.
[7] I. N. Stranski, Z. Phys. Chem. **136**, 259 (1928).
[8] M. A. Lovette, A. R. Browning, D. W. Griffin, J. P. Sizemore, R. C. Snyder, and M. F. Doherty, Industrial & Engineering Chemistry Research **47**, 9812 (2008).
[9] H. M. Cuppen, H. Meekes, W. J. P. v. Enckevort, G. W. M. Vissers, and E. Vlieg, Surface Science **569**, 33 (2004).
[10] P. Bennema, Journal of Physics D: Applied Physics **26**, B1 (1993).
[11] X.-Y. Liu and P. Bennema, J. Cryst. Growth **139**, 179 (1994).
[12] R. A. Laudise, Journal of the American Chemical Society **81**, 562 (1959).
[13] S. Gorti, E. L. Forsythe, and M. L. Pusey, Acta Crystallogr. Sect. D-Biol. Crystallogr. **61**, 837 (2005).
[14] H.-C. Jeong and E. D. Williams, Surface Science Reports **34**, 171 (1999).
[15] X.-Y. Liu, P. van Hoof, and P. Bennema, Physical Review Letters **71**, 109 (1993).
[16] B. Mutaftschiev, *The atomistic nature of crystal growth* (Springer, Berlin, Heidelberg, 2001).

[17] F. Spaepen, in *Solid State Physics, Vol. 47* (Academic Press, Boston, 1994), pp. 1.
[18] W. K. Burton, Cabrera, N. &. Frank, F.C., *Phil. Trans. Roy. Soc. London Ser. A* **243**, 299 (1951).
[19] K. A. Jackson, in *Growth and Perfection of Crystals*, edited by R. H. Doremus, B. W. Roberts, and D. Turnbull (Chapman and Hill, London, 1958), pp. 319.
[20] I. V. Markov, *Crystal Growth for Beginners: Fundamentals of Nucleation, Crystal Growth and Epitaxy* (WORLD SCIENTIFIC Publishing Company Incorporated, 2016).
[21] T. Halpin-Healy and Y.-C. Zhang, Physics Reports **254**, 215 (1995).
[22] S. Majaniemi, T. Ala-Nissila, and J. Krug, Physical Review B **53**, 8071 (1996).
[23] P. G. Vekilov, J. D. Rimer, K. Olafson, and M. Ketchum, CrystEngComm **17**, 7790 (2015).
[24] K. N. Olafson, M. A. Ketchum, J. D. Rimer, and P. G. Vekilov, Proceedings of the National Academy of Sciences **112**, 4946 (2015).
[25] M. A. Ketchum, K. N. Olafson, E. V. Petrova, J. D. Rimer, and P. G. Vekilov, The Journal of Chemical Physics **139**, 121911 (2013).
[26] D. J. Sullivan, Int J Parasitol **32**, 1645 (2002).
[27] A. P. Gorka, A. de Dios, and P. D. Roepe, Journal of Medicinal Chemistry **56**, 5231 (2013).
[28] L. A. M. J. Jetten, H. J. Human, P. Bennema, and J. P. Van Der Eerden, J. Cryst. Growth **68**, 503 (1984).
[29] H. M. Cuppen, H. Meekes, W. J. P. van Enckevort, E. Vlieg, and H. J. F. Knops, Physical Review B **69**, 245404 (2004).
[30] M. Elwenspoek and J. P. v. d. Eerden, Journal of Physics A: Mathematical and General **20**, 669 (1987).
[31] E. van Veenendaal, P. J. C. M. van Hoof, J. van Suchtelen, W. J. P. van Enckevort, and P. Bennema, Surface Science **417**, 121 (1998).
[32] K. N. Olafson, M. A. Ketchum, J. D. Rimer, and P. G. Vekilov, Crystal Growth & Design **15**, 5535 (2015).
[33] S. Pagola, P. W. Stephens, D. S. Bohle, A. D. Kosar, and S. K. Madsen, Nature **404** 307 (2000).
[34] T. Michely and J. Krug, *Islands, Mounds and Atoms. Patterns and Processes in Crystal Growth Far from Equilibrium* (Springer, Heidelberg, Germany, 2004).
[35] L. Onsager, Physical Review **65**, 117 (1944).
[36] P. Nozières and F. Gallet, J. Phys. France **48**, 353 (1987).
[37] S. Gorti, E. L. Forsythe, and M. L. Pusey, Crystal Growth & Design **4**, 691 (2004).
[38] I. Reviakine, W. Bergsma-Schutter, and A. Brisson, Journal of Structural Biology **121**, 356 (1998).
[39] S.-T. Yau, D. N. Petsev, B. R. Thomas, and P. G. Vekilov, J. Mol. Biol. **303**, 667 (2000).
[40] K. Binder, in *Phase Transformations of Materials*, edited by P. Haasen (VCH Verlag, Weinheim, 1990).
[41] K. Binder and P. Fratzl, in *Phase Transformation in Materials*, edited by G. Kostorz (Wiley, New York, 2001).
[42] P. G. Debenedetti, *Metastable Liquids* (Princeton Univ Pr, Princeton, 1996).
[43] M. Shah, O. Galkin, and P. G. Vekilov, J. Chem. Phys. **121**, 7505 (2004).
[44] A. A. Chernov, Annual Review of Materials Science **3**, 397 (1973).
[45] W. van Saarloos and G. H. Gilmer, Physical Review B **33**, 4927 (1986).

[46] M. Prähofer and H. Spohn, Physical Review Letters **84**, 4882 (2000).
[47] M. Sleutel, D. Maes, L. Wyns, and R. Willaert, Crystal Growth & Design **8**, 4409 (2008).
[48] P. G. Vekilov, Crystal Growth and Design, **7**, 2796 (2007).
[49] P. G. Vekilov, L. A. Monaco, and F. Rosenberger, J. Crystal Growth **156**, 267 (1995).
[50] O. Galkin and P. G. Vekilov, J. Amer. Chem. Soc. **122**, 156 (2000).
[51] M. Sleutel, R. Willaert, C. Gillespie, C. Evrard, L. Wyns, and D. Maes, Crystal Growth & Design **9**, 497 (2009).
[52] C. R. Chong and D. J. Sullivan Jr, Biochemical Pharmacology **66**, 2201 (2003).
[53] K. N. Olafson, T. Q. Nguyen, J. D. Rimer, and P. G. Vekilov, Proceedings of the National Academy of Sciences **114**, 7531 (2017).
[54] D. E. Goldberg, A. F. Slater, A. Cerami, and G. B. Henderson, Proceedings of the National Academy of Sciences **87**, 2931 (1990).
[55] A. U. Orjih, H. S. Banyal, R. Chevli, and C. D. Fitch, Science **214**, 667 (1981).

[56] R. Kaischew, Z. Phys. 102, 684 (1936).
[57] R. Kaischew and I. N. Stranski, Z. Phys. Chem. B35, 427 (1937).
[58] D. S. Bohle, R. E. Dinnebier, S. K. Madsen, and P. W. Stephens, Journal of Biological Chemistry 272, 713 (1997).
[59] B. Mutaftschiev, The atomistic nature of crystal growth (Springer, Berlin, Heidelberg, 2001).
[60] D. Turnbull, Journal of Applied Physics 21, 1022 (1950).

Figure captions

Fig. 1 (color online). Rough and smooth crystal interfaces, illustrated in (a) and (b), respectively. A kink is highlighted in red and a step edge, in blue. (c) – (f) Steady-state morphology of (100) hematin faces, imaged in phase mode, at four hematin concentrations c_H and corresponding supersaturations $\Delta\mu/k_BT$. At low c_H and $\Delta\mu$, in (c), hematin crystals grow by the generation and spreading of layers. At higher c_H and $\Delta\mu$ in (d) to (f), the surface is rough.

Fig. 2 (color online). The hematin surface roughness. (a) and (b) Schematics of kinetic roughening at increasing supersaturation $\Delta\mu$ by (a) denser 2D nucleation and (b) higher step density in a step train. The radius of a 2D island R is illustrated in (a) and a step width w, inter-step separation $\boldsymbol{\ell}$, and correlation length ξ in (b). (c) – (f) The distribution of the mean squared roughness R_q for 100×100 nm^2 areas at four $\Delta\mu$ values, corresponding to the images in Fig. 1 (c) – (f). (g) Average R_q computed from the data in (c) – (f) as a function of $\Delta\mu$. Range of rough growth shaded in grey.

Fig. 3 (color online). The critical 2D nucleus radius R_c and the step width w. (a) – (f) Illustration of the determination of R_c at c_H = 0.21 mM and $\Delta\mu = 0.27k_BT$ from the size and shape fluctuations of a newly nucleated island, indicated by the arrow in (b). (g) The dependence of R_c on the supersaturation $\Delta\mu$ [24]. The solid line denotes the predicted $R_c = \gamma\Omega/\Delta\mu$ dependence. The shaded area denotes the region of rough growth. A horizontal dashed line marks the value of R_c

at the roughening transition. (h) A high resolution image of a step edge at c_H = 0.28 mM, highlighted with a white contour; w is indicated.

Fig. 4 (color online). The normal growth rate V and the overlapping of step supply fields. (a) – (e) A sequence of *in situ* AFM images of a (100) face, recorded at c_H = 0.23 mM, displaying the growth of two steps (left and right) in opposing directions. (f) V of (100) faces determined as discussed in the SM at [URL will be inserted by publisher]. The face kinetic coefficient β_{face} is defined as the slope of the $V(c_H - c_e)$ correlation.

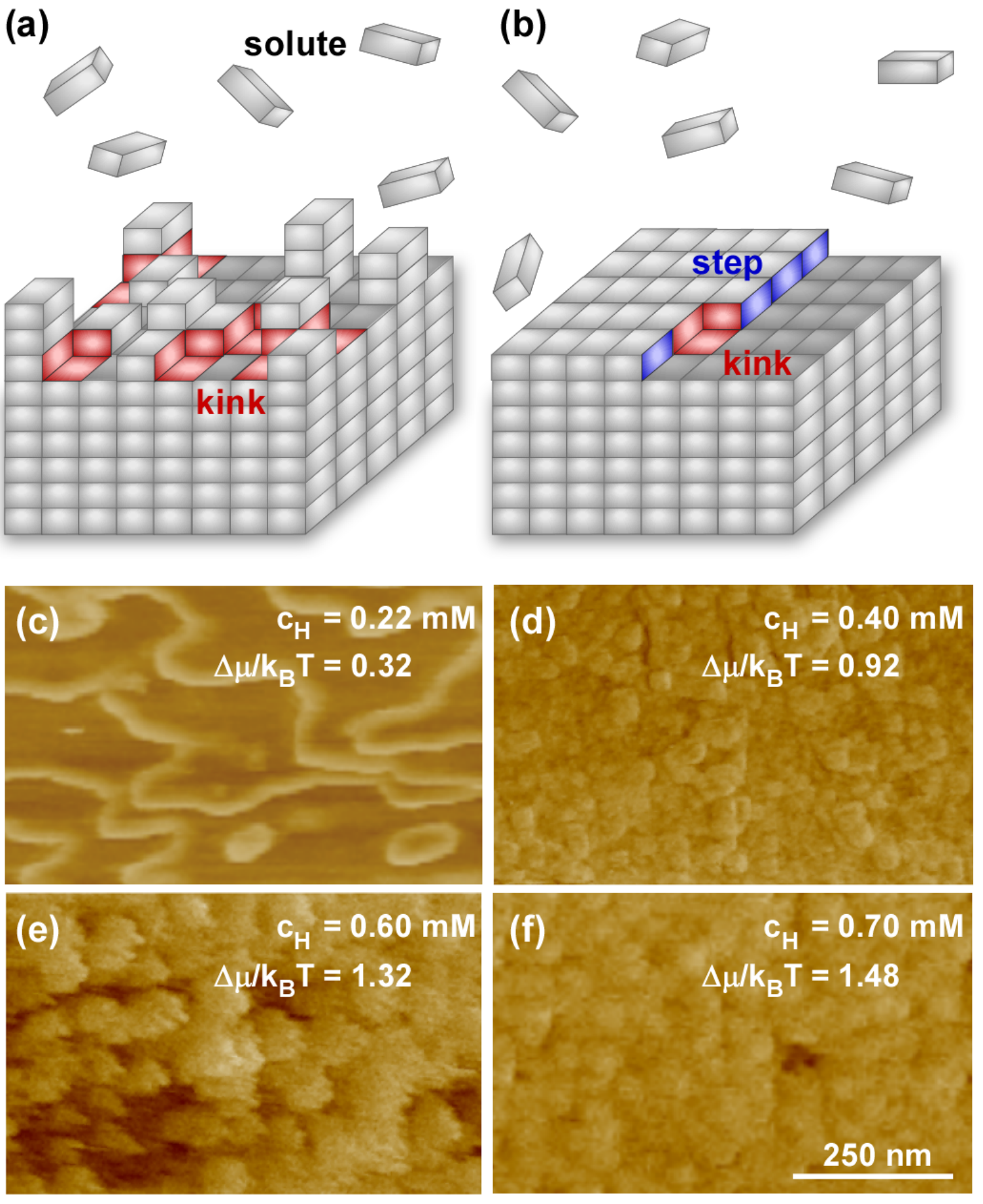
(a)
solute
kink
(b)
step
kink
(c)
c_H = 0.22 mM
$\Delta\mu/k_BT$ = 0.32
(d)
c_H = 0.40 mM
$\Delta\mu/k_BT$ = 0.92
(e)
c_H = 0.60 mM
$\Delta\mu/k_BT$ = 1.32
(f)
c_H = 0.70 mM
$\Delta\mu/k_BT$ = 1.48
250 nm

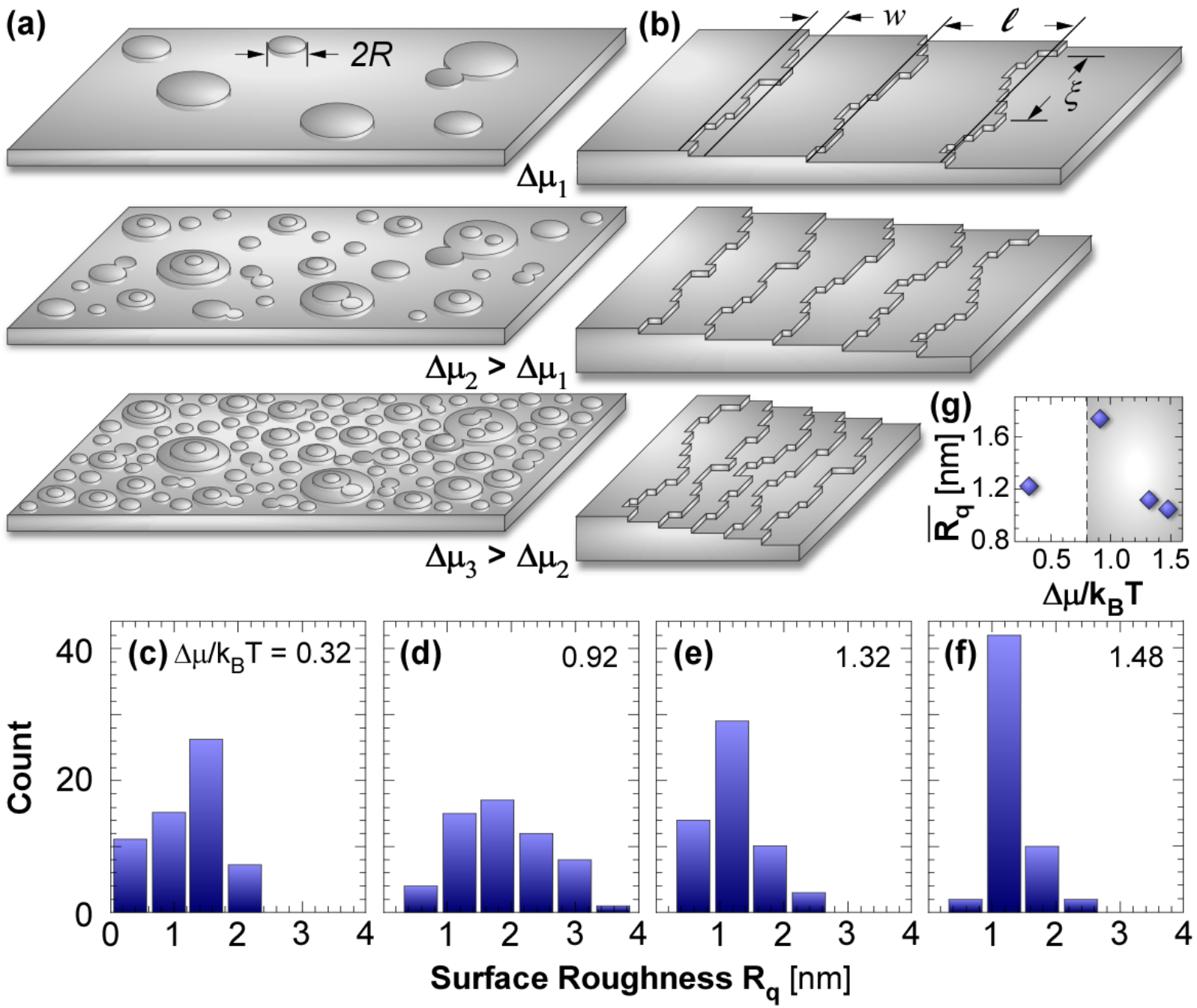
(a)
2R
(b)
w
ℓ
ξ
Δμ1
Δμ2 > Δμ1
Δμ3 > Δμ2
(g)
1.6
1.2
0.8
R̄q [nm]
0.5
1.0
1.5
Δμ/kBT
(c) Δμ/kBT = 0.32
(d) 0.92
(e) 1.32
(f) 1.48
40
20
0
Count
0
1
2
3
4
Surface Roughness Rq [nm]

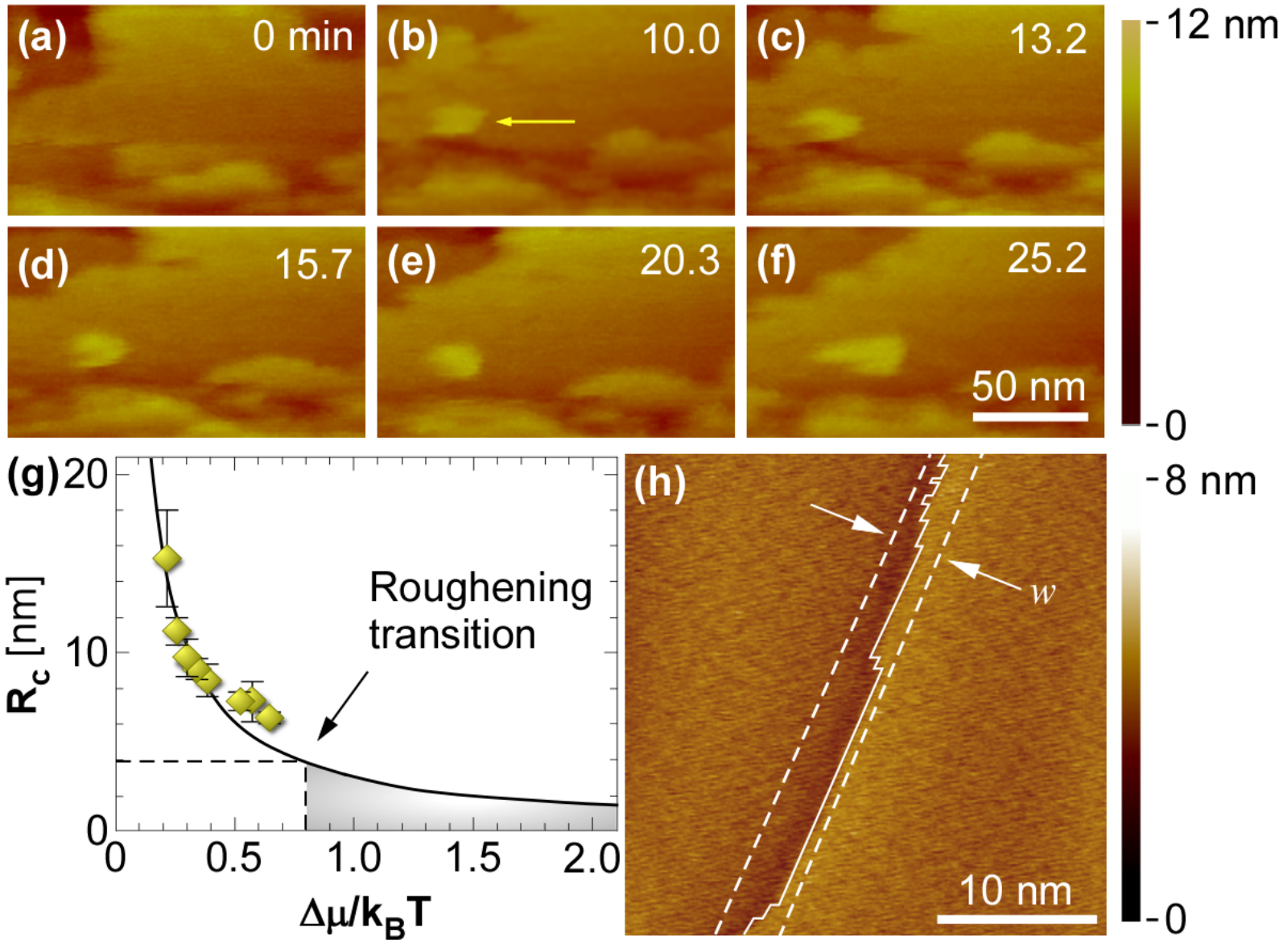
(a)
0 min
(b)
10.0
(c)
13.2
(d)
15.7
(e)
20.3
(f)
25.2
50 nm
12 nm
0
(g)
20
10
0
R_c [nm]
0
0.5
1.0
1.5
2.0
$\Delta\mu/k_BT$
Roughening transition
(h)
w
10 nm
8 nm
0

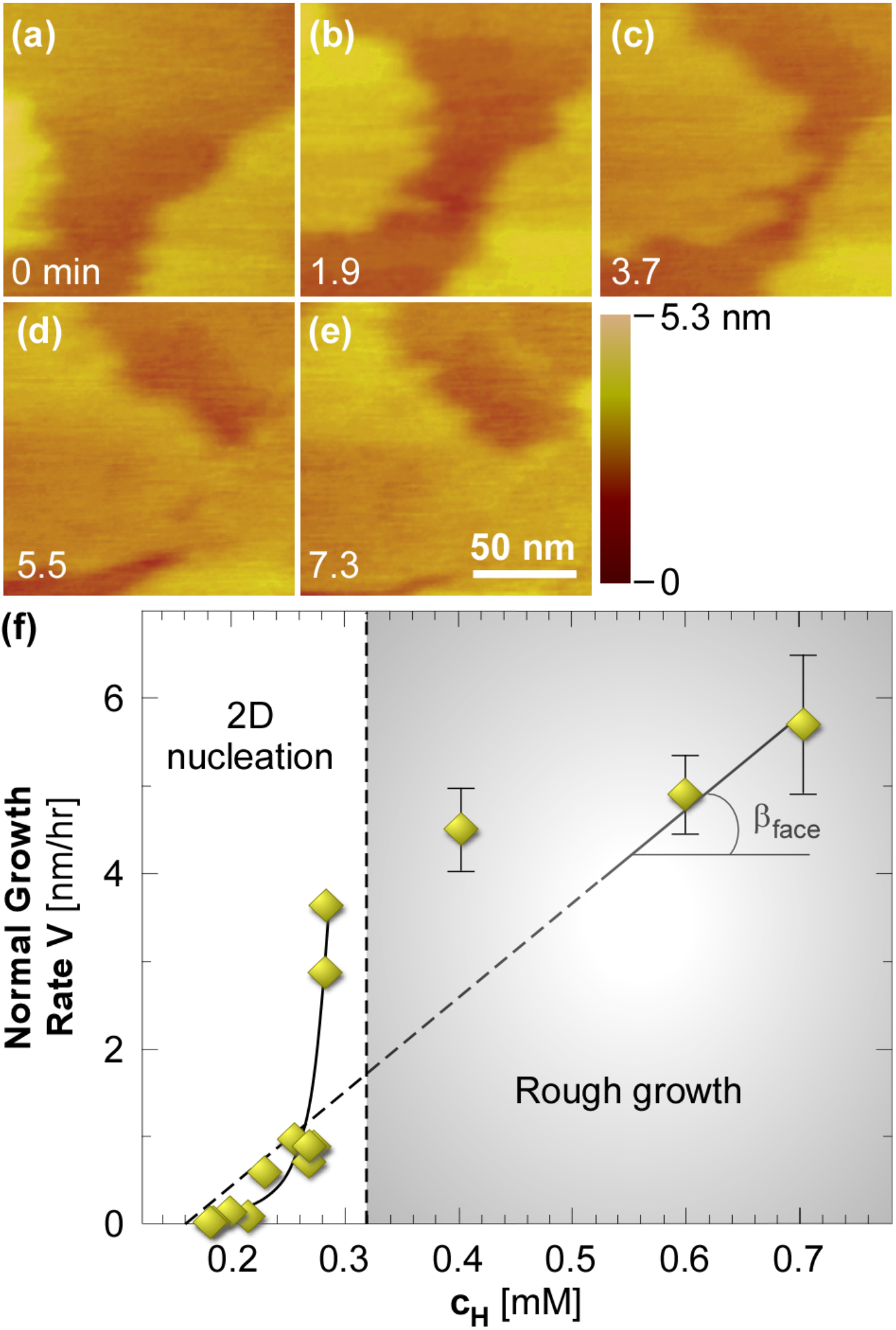
(a)
0 min
(b)
1.9
(c)
3.7
(d)
5.5
(e)
7.3
50 nm
5.3 nm
0
(f)
2D
nucleation
Rough growth
β_{face}
Normal Growth
Rate V [nm/hr]
0
2
4
6
0.2
0.3
0.4
0.5
0.6
0.7
c_H [mM]